Equivalent seismic coefficients for caisson foundations supporting bridge piers

D. Gaudio[a, 1], S. Rampello[b]

[a] Dipartimento di Ingegneria Strutturale e Geotecnica, Università di Roma *La Sapienza*, Via Eudossiana 18, 00184 Roma, Italy

Corresponding Author

Prof. Sebastiano Rampello

sebastiano.rampello@uniroma1.it

Tel: +39 06 44585 989

E-mail addresses:

dg564@cam.ac.uk [1]*(D. Gaudio), sebastiano.rampello@uniroma1.it (S. Rampello).*

[1] Present Address: Department of Engineering, University of Cambridge, Trumpington Street, Cambridge, CB21PZ, UK

ABSTRACT

Safety of a foundation under seismic loading is strongly dependent on the inertial forces transmitted by the superstructure, exchanged with the surrounding soil and acting into the foundation itself. The latter contribution, typically neglected for shallow and pile foundations, should be considered for caisson foundations, much more massive and rigid than the foundation soil. In this paper, the inertial forces acting in caisson foundations during seismic shaking are extracted from the results of a parametric study where different caissons supporting bridge piers are subjected to severe ground motions. The parametric study was carried out in the time domain via 3D Finite Element (FE) dynamic analyses performed in terms of effective stresses but assuming an undrained response of the foundation soil. Non-linear and inelastic soil behaviour was described in the analyses by an elastic-plastic constitutive model with isotropic hardening.

In the framework of a pseudo-static approach, the caisson inertia is represented by equivalent horizontal and rotational seismic coefficients, $k_{\mathrm{h\,eq}}$ and $k_{\mathrm{rot\,eq}}$, relating the generalised inertial forces to the caisson weight. The coefficient $k_{\mathrm{h\,eq}}$ turns out to be always remarkably smaller than the maximum value computed at ground surface in free-field conditions, $k_{\mathrm{h\,max}}^{(\mathrm{g.s.})}$. The equivalent seismic coefficients $k_{\mathrm{h\,eq}}$ and $k_{\mathrm{rot\,eq}}$ are expressed via empirical relationships as a function of the dynamic properties of the whole system and the seismic input, through dimensionless parameters. Calculation examples are finally given, where safety assessment of bearing capacity is made for different systems using the pseudo-static approach, showing that use of the seismic coefficients computed by the proposed relationships yields results consistent with the ones obtained from the dynamic analyses.

Keywords: Horizontal seismic coefficient, Rotational seismic coefficient, Pseudo-static approach, Caisson foundations, Bridge piers, Bearing capacity, 3D dynamic analyses, Soil-structure interaction

1. Introduction

Earthquake-induced accelerations produce inertial forces in foundation structures, adding to their self-weight and thus bringing them closer to one or more of its limit states, represented by either bearing capacity or pure-sliding resistance. These inertial actions cannot be neglected for caisson foundations supporting long-span bridge piers, as frequently done for shallow or pile foundations, in that caissons are typically much more massive and rigid than the surrounding foundation soil. When considering foundation inertia, reference is made to the horizontal acceleration at ground surface or foundation level in free-field conditions for shallow foundations, this assumption being not suitable for embedded massive caisson foundations as they would be excessively loaded.

In the absence of liquefaction phenomena, safety assessment of foundations subjected to seismic loadings can be checked in the framework of the Performance-Based Design approach (PBD), computing maximum and permanent values of the horizontal displacements, settlements and/or rotations attained during and at the end of the seismic event and comparing them to given threshold values related to the considered limit state. While no application of this approach can be found in the literature for caisson foundations, this has been increasingly applied to shallow foundations, through macro-element formulations [e.g: 1-6] or Newmark-type calculations [7]. However, due to the inherent difficulty in finding appropriate input time histories, common practice still relies on the pseudo-static approach, where foundation inertia is represented by equivalent static forces proportional to the caisson self-weight via the seismic coefficient *k*. This approach has been widely adopted for shallow foundations [8-12] considering the inertial forces applied to the superstructure and the soil, but ignoring the foundation inertia. Izumi and Miura [13] provided an estimation of the foundation inertial actions through the

horizontal seismic coefficient k of embedded foundations of building structures. Soil-structure interaction effects were considered, while neither the possible development of irreversible strains in the foundation soils nor the rotational component of motion of the embedded foundations were accounted for in calculations.

Inertial forces acting in caisson foundations supporting bridge piers depend on kinematic and inertial interactions, that is on the inertial forces acting in the foundation soil and in the superstructure, as well as on the irreversible and hysteretic soil behaviour. Kinematic effects of caisson foundations, that is the inertial forces applied to the foundation soil, typically contribute to reduce the horizontal acceleration while introducing an angular acceleration of the caisson [14-16], due to the high impedance ratio between the caisson and the soil. Inertial and kinematic effects, together with free-field propagation of high-intensity seismic waves may bring the foundation soil to a plastic regime limiting the forces that can be exchanged between the soil and the caisson [17, 18]. All these phenomena occur simultaneously, making the evaluation of the inertial forces acting in the caisson complex, this requiring time-consuming numerical analyses.

In this paper, the horizontal and rotational seismic coefficients, k_h and k_{rot}, to be used in a pseudo-static safety assessment of caisson foundations supporting bridge piers, are derived using the results of a parametric study where different soil-caisson-pier-deck systems were subjected to several strong ground motions, capable of triggering plastic mechanisms for the soil-caisson systems [17, 19]. The 3D FE dynamic analyses were carried out in the time domain accounting for the non-linear and irreversible soil behaviour starting from small-strain levels, using an elastic-plastic constitutive model. The equivalent seismic coefficients $k_{h\ eq}$ and $k_{rot\ eq}$ are assumed equal to the peak values of the relevant time histories. They are related to non-dimensional parameters expressing

the dependence of the inertial forces on the dynamic properties of the compliant-base system and of the seismic input, thus giving some insight into the parameters controlling the foundation inertia. Empirical relationships are therefore derived, that provide a simplified though useful tool to estimate the equivalent seismic coefficients. Two calculation examples are also illustrated where the pseudo-static approach is applied to a stiff and a flexible soil-foundation-superstructure system, showing how to compute the seismic coefficients and how much they affect the caisson safety against bearing capacity.

2. Problem definition

The scheme adopted for the pseudo-static evaluation of the bearing capacity $N_{\mathrm{lim,e}}$ of caisson foundations supporting bridge piers is shown in Fig. 1. A cylindrical caisson of height H and diameter D is subjected in limit conditions to: the resultant loading transmitted to the head of the caisson by the superstructure, that is the vertical limit force $N_{\mathrm{head,lim}}$, the horizontal load Q_{s} and the moment M_{s} (*superstructure inertia*); the earth pressure applied by the surrounding soil at the lateral surface and at the base of the caisson, with resultant forces $S_{1,\mathrm{e}}$ for $z \leq z_{\mathrm{r}}$, $S_{2,\mathrm{e}}$ for $z \geq z_{\mathrm{r}}$, $N_{\mathrm{lim,e}}$ and $Q_{\mathrm{lim,e}}$ for $z = H$, where the subscript "e" indicates that these forces depend on the acceleration propagating in the foundation soil (*soil inertia*); and the inertial forces acting in the caisson, whose resultant are expressed by the vertical load $k_{\mathrm{v\,eq}} \cdot W_{\mathrm{c}}$, the horizontal load $k_{\mathrm{h\,eq}} \cdot W_{\mathrm{c}}$ and the moment $k_{\mathrm{rot\,eq}} \cdot W_{\mathrm{c}} \cdot D$, where W_{c} is the self-weight of the caisson and $k_{\mathrm{v\,eq}}$, $k_{\mathrm{h\,eq}}$ and $k_{\mathrm{rot\,eq}}$ are the equivalent vertical, horizontal and rotational seismic coefficients (*foundation inertia*).

In the pseudo-static approach, the equivalent static forces representing the foundation inertia are applied at the caisson centroid (G) and are assumed constant with time. In this work, for the sake of simplicity, the contribution of vertical acceleration on the inertial

forces acting in the caisson is neglected ($k_{v\,eq} = 0$), similarly to [12] for shallow foundations, though Cascone and Casablanca [10] showed that the effect of the vertical pseudo-static force may be significant depending on the adopted value of $k_{v,eq}$.

In Fig. 1 a specific collapse mechanism is assumed where the caisson rotation pole (O) is located at a depth $z_r < H$. This is the prevailing failure mode for caissons supporting bridge piers when two conditions are met: the first mode of the pier is predominant, thus transmitting about in-phase horizontal and moment loads to the caisson, and the kinematic constraint imposed by the deck to the bridge pier is negligible [20, 21]. However, the above-listed system of forces is general and still valid for a different location of the rotation pole.

Time histories of both the horizontal and the rotational seismic coefficients, $k_h(t)$ and $k_{rot}(t)$, are computed referring to the results of a parametric study carried out by Gaudio and Rampello [17] where different cylindrical caisson foundations supporting bridge piers were subjected to severe seismic inputs. The schematic layout of the problem considered in the parametric study is shown in Fig. 2a: the caissons supporting bridge piers of height h_s are embedded in a 5-meter-thick sandy layer that is underlain by a 55-meter-thick layer of silty clay. The assumed profiles of overconsolidation ratio *OCR* and small-strain shear modulus G_0 are plotted in Fig. 2b. Initial pore water pressure regime is hydrostatic with the water table at depth $z_w = 5$ m. The seismic inputs were applied in the x direction at the bedrock depth in terms of horizontal acceleration time histories, this corresponding to assume a rigid bedrock. Neither the interaction between two contiguous piers nor the transversal and torsional stiffness of the deck were taken into account in the study referring to long span bridges. The pier and the caisson were assimilated to a

viscous-elastic medium. The pier was modelled as a Single Degree of Freedom system (SDoF) characterised by a lumped mass m_s, a (flexural) stiffness k_s and a damping ratio ξ_s = 5 %, where the lumped mass m_s encompasses both the deck and the upper half of the pier ($m_s = m_{deck} + 0.5 \cdot m_{pier}$), while the weight of the lower half of the pier was applied at the caisson head through a vertical stress $\sigma_{z\,(0.5pier)}$ to reproduce correctly the initial stress state in the foundation soil.

Soil behaviour was described through the *Hardening Soil with Small-Strain Stiffness* constitutive model (*HSsmall*, [22]), available in the Plaxis 3D suite [23], an elastic-plastic model with isotropic hardening and Mohr-Coulomb failure criterion. The main parameters assumed in the analyses are listed in Tab. 1, where γ is the unit weight, c' and φ' are the effective cohesion and angle of shearing resistance, k_0 is the earth pressure coefficient at rest, G_0^{ref} and m are model parameters whose values were determined to reproduce the G_0 profile of Fig. 2b, $\gamma_{0.7}$ is the shear strain corresponding to a decay of the secant shear modulus $G_s/G_0 = 0.722$, and E_{ur}^{ref} is the unloading-reloading Young's modulus at a reference pressure p_{ref} = 100 kPa. The remaining parameters of the *HSsmall* model were defined in the analyses using default values, as it follows: Poisson's ratio $\nu_{ur} = 0.2$ and elastic-plastic moduli $E_{50}^{ref} = E_{oed}^{ref} = E_{ur}^{ref}/3$.

Fig. 3a-d shows the 6 time histories of horizontal acceleration of real records, preliminarily amplified to obtain given values of Arias intensity I_A^{inp} [24] and selected to match a site-specific spectrum obtained for: a 10 % probability of exceedance (Ultimate Limit State); a design working life V_N = 100 years (return period T_R = 1424 years); a subsoil class C ($V_{S,\,30}$ = 204 m/s) and a damping ratio equal to that assumed for the pier, $\xi = \xi_s$ = 5 %. The ground motions were grouped in 2 sets differing in the values of Arias

intensity, I_A^{inp} = 1.12 ÷ 1.17 m/s and I_A^{inp} = 2.79 ÷ 2.87 m/s. Tab. 2 lists the main ground motion parameters of the 6 records, where F is the amplification factor by which the seismic input motions were multiplied to obtain the desired values of the Arias intensity, a_{max}^{inp} is the peak horizontal acceleration, T_m^{inp} is the mean period [25] and T_D^{inp} is the significant duration [26]. These records were selected to cover a wide range of frequency contents and strong-motion durations as well as to be intense enough to promote the activation of plastic strains in the foundation soil. With respect to the records on the first row of each set of Tab. 2 (Tolmezzo E-W and Colfiorito N-S), the acceleration time histories listed on the second row (Assisi E-W and Nocera Umbra N-S) are characterised by a halved mean period T_m^{inp}, this corresponding to Fourier spectra rich in high frequencies, as depicted in Fig. 3c-f. Similarly, the time histories related to the third row of each set in Tab. 2 (Adana E-W and Dayhook N-S) show a larger duration T_D^{inp}, equal to about 2.5 times that of Tolmezzo and Colfiorito records (Fig. 3b-e).

In the parametric study, 14 deck-pier-caisson-soil systems were subjected to the 3 seismic inputs of the first set of accelerograms, the systems differing in caisson diameter (D = 8 and 12 m), caisson slenderness ratio (H/D = 0.5, 1 and 2) and pier height (h_s = 15, 30 and 60 m), while the seismic inputs of the second set were applied to systems with D = 12 m and h_s = 30 m only, this returning 51 performed analyses.

The system properties are listed in Tab. 3, where k_s and m_s are the stiffness and the lumped mass of the SDoF representing the piers and T_{eq} is the equivalent fundamental period, related to the first mode of the compliant-base system, evaluated using the empirical relationship proposed by Tsigginos *et al*. [27]:

$$\frac{T_{eq}}{T_s} \approx 1 + \left(\frac{2\pi}{T_s} \cdot \frac{h_s}{V_{S,eq}} \right)^{1.18} \left(\frac{m_s}{m_c} \right)^{0.613} \left(2\frac{h_s}{D} \right)^{-0.5} \quad (1)$$

where T_s is the period of the fixed-base system, $V_{S,eq}$ is the equivalent shear wave velocity of the soil interacting with the foundation, and m_c is the caisson mass. Gaudio and Rampello [28] recently showed a fair agreement between the periods T_{eq} provided by the Tsigginos et al. [27] relationship and those computed by non-linear FE dynamic analyses. Specifically, slightly higher values of T_{eq} were obtained using eq. (1), with a maximum error smaller than 25 % and a mean error equal to 12 %.

These properties are representative of simple and continuous-spanned bridges with span length of 40 to 110 m: they were selected to return given safety factors against bearing capacity under static and pseudo-static conditions, F_{Sv} = 5.5 and F_{Se} = 0.7, the former selected to reproduce conditions usually met in common practice, while the latter adopted to promote the activation of plastic strains during the seismic event [29]. Safety factors were calculated using classical solutions [30, 31] for the evaluation of the bearing capacity under static and pseudo-static conditions. All the systems are then characterised by the same degree of shear strength mobilisation prior to applying the seismic input [17].

The 3D FE model used in the parametric study is shown in Fig. 2c. Half of the domain is modelled thanks to the symmetry of the problem at hand. Mesh coarseness was set by performing preliminary sensitivity analyses until the model provided mesh-independent results. The pier and the lumped mass are represented by linear viscous-elastic one-dimensional beam elements, the pier being modelled by a zero-mass-density element. Foundation soils are modelled through homogeneous soil strata, to reproduce the profiles of *OCR* and G_0 plotted in Fig. 2b. Interface elements described the soil-caisson contact to

simulate possible non-linear phenomena such as relative sliding. Before the concrete caisson elements were activated, a volumetric contraction was applied to the caisson volume to simulate shaft excavation prior to caisson construction, thus attaining active limit conditions in the soil next to the caisson. The caisson and the superstructure were then both activated assuming drained conditions for soils. Undrained conditions were instead assumed in the dynamic phase, running a consolidation analysis at its end to dissipate the excess pore water pressure cumulated during the seismic shaking.

More details on the FE model, the calibration of input parameters, as well as the properties of the studied systems are given in [17] and [32].

3. Evaluation of seismic coefficients

The horizontal and rotational seismic coefficients, k_h and k_{rot}, represent the inertial forces acting in the foundation during the seismic event. Should the caisson have the same inertial and stiffness properties of the foundation soil, the forces exchanged between the caisson and the soil in the absence of the superstructure would be null and the seismic-induced inertial actions would be entirely balanced by the horizontal force acting at the caisson base. Indeed, in these conditions the caisson could be considered as a volume of soil in free-field conditions (*ff*). However, as the caisson is characterised by a density ρ_c and a Young's modulus E_c different from the ones of the soil, ρ and E, some horizontal forces and moments arise at the soil-caisson contact at every time instant t. These generalised forces are $\Delta Q(t) = Q_c(t) - Q_{ff}(t)$ and $\Delta M(t) = M_c(t) - M_{ff}(t)$, where Q and M are the horizontal forces and the moments acting in the caisson (*c*) and in the soil (*ff*). Under 1D conditions it is $M_{ff} = 0$ and the seismic coefficients can be expressed as it follows:

$$k_h(t) = \frac{\Delta Q(t)}{W_c} = -\frac{m_c \cdot a_c(t) - m_{ff} \cdot a_{ff}(t)}{W_c} \tag{2}$$

$$k_{rot}(t) = \frac{\Delta M(t)}{W_c \cdot D} = -\frac{J_c \cdot \ddot{\theta}_c(t)}{W_c \cdot D} \tag{3}$$

where $W_c = m_c \cdot g$ is the caisson weight, m_c and m_{ff} are the masses of the caisson and the soil, $a_c(t)$ and $a_{ff}(t)$ are the horizontal accelerations time histories acting in the caisson and the soil, J_c and $\ddot{\theta}_c(t)$ are the rotational inertia and the angular acceleration time history of the caisson.

Time histories of seismic coefficients $k_h(t)$ and $k_{rot}(t)$ were extracted from the results of the parametric study mentioned above [17], referring to the scheme plotted in Fig. 4. The caisson was divided in n disks of equal height (h_i = 2 m) and the time histories of horizontal acceleration were computed at the depth of each disk's centroid, for both the caisson and the soil in free-field conditions. Adapting eqs. (2) and (3) to the discretised caisson and soil volume and substituting the expressions of caisson weight and rotational inertia, $W_c = \rho_c \cdot g \cdot [\pi D^2/4 \cdot H]$ and $J_c = W_c/[12g] \cdot [3(D/2)^2 + H^2]$, where ρ_c = 2.55 Mg/m^3 is the density of reinforced concrete, the following relationships are obtained for the seismic coefficients:

$$k_h(t) = -\frac{\sum_{i=1}^{n}\left[\frac{a_c(z_i,t)}{g} - \frac{\rho}{\rho_c}\frac{a_{ff}(z_i,t)}{g}\right] \cdot h_i}{H} \tag{4}$$

$$k_{rot}(t) = -\frac{D}{12g}\left[\frac{3}{4} + \left(\frac{H}{D}\right)^2\right] \cdot \ddot{\theta}_c(t) \tag{5}$$

where the horizontal accelerations of the caisson and the soil, at depth z_i, are $a_c(z_i, t)$ and $a_{ff}(z_i, t)$, the gravitational acceleration is g = 9.81 m/s^2 and the angular acceleration of the

caisson is $\ddot{\theta}_c(t) = \left[a_c(z=0,t) - a_c(z=H,t)\right]/H$. Fig. 5 shows the profiles of horizontal acceleration computed in the caisson (Fig. 5a) and in the soil in free-field conditions (Fig. 5b), for the specific case of a bridge pier of height h_s = 30 m supported by a caisson with diameter D = 12 m and slenderness ratio H/D = 2, subjected to the Adana record. Results are depicted at the time instants when the Arias intensity of the input motion is equal to I_A^{inp} = 5, 70, 90 and 99 % of its maximum. Acceleration profiles are always linear with depth in the caisson, irrespective of the considered alignment, this showing the caisson behaving as a rigid body due to its stiffness much higher than that of the soil. The profiles of caisson and soil accelerations, computed for I_A^{inp} = 70 % (t = 11.705 s) are plotted in Fig. 6a, the shaded area representing the relative acceleration (a_c - a_{ff}), while the term in square brackets of eq. (4) is plotted in Fig. 6b and adopted to evaluate the horizontal seismic coefficient, k_h (t = 11.705 s) = 0.040. Fig. 6c shows the constant angular acceleration of the caisson $\ddot{\theta}_c(t = 11.705\text{ s}) \approx 0.01\text{rad/s}^2$, this providing a value k_{rot} (t = 11.705 s) = 0.005 for the rotational seismic coefficient.

The calculation of the seismic coefficients was performed at every time instant, obtaining the time histories $k_h(t)$ and $k_{rot}(t)$ plotted in Fig. 7. In the following, the mean period and Arias Intensity of $k_h(t)$ are denoted as $T_m^{(h)}$ and $I_A^{(h)}$, while the ones for $k_{rot}(t)$ are $T_m^{(rot)}$ and $I_A^{(rot)}$.

The earthquake-induced generalised forces ΔQ and ΔM acting at the caisson centroid, at depth $z = z_G = H/2$, can be evaluated from the time histories of the seismic coefficients. They can be added, at every time instant, to those transmitted to the caisson head by the superstructure, Q_s and M_s, to obtain the resulting forces acting in the caisson. To this end, taking as Load Reference Point (*LRP*) the centroid of the top section of the caisson (z = 0),

the following total generalised forces are obtained:

$$Q_{\mathrm{tot}}(t) = Q_{\mathrm{s}}(t) + \Delta Q_{\mathrm{head}}(t) = Q_{\mathrm{s}}(t) + \left[k_{\mathrm{h}}(t) \cdot W_{\mathrm{c}}\right] \tag{6}$$

$$M_{\mathrm{tot}}(t) = M_{\mathrm{s}}(t) + \Delta M_{\mathrm{head}}(t) = M_{\mathrm{s}}(t) + k_{\mathrm{h}}(t) \cdot W_{\mathrm{c}} \cdot \frac{H}{2} - k_{\mathrm{rot}}(t) \cdot W_{\mathrm{c}} \cdot D \tag{7}$$

The generalised inertial forces Q_{tot} and M_{tot} computed for the system and the input of Figs. 5-7 are plotted in Fig. 8 in terms of loading paths (M_{tot} - Q_{tot}) and (M_{s} - Q_{s}), that is with and without considering foundation inertia. The pseudo-static interaction domain shown in the figure was computed from monotonic undrained pushover analyses assuming the limit state be reached when the tangent stiffness of load-displacement curves reduces to 1 % of the initial stiffness [33]. The interaction domain was computed assuming a constant seismic coefficient in the soil, taken as that calculated in free field at the same time instant for which the maximum moment acting in the foundation is attained ($k_{\mathrm{h\ soil}}$ = 0.171).

The influence of foundation inertia is clearly visible comparing the M_{tot} - Q_{tot} loading paths with those described by the superstructure loads only (Q_{s}, M_{s}) (Fig. 8). Although limit conditions are attained both with and without considering the foundation inertial forces, peak values of total and superstructure forces are quite different. Specifically, $|Q_{\mathrm{s}}|_{\max}$ = 20.7 MN and $|M_{\mathrm{s}}|_{\max}$ = 621.6 MN·m are computed without considering the foundation inertia, whereas peak values $|Q_{\mathrm{tot}}|_{\max}$ = 27.8 MN and $|M_{\mathrm{tot}}|_{\max}$ = 655.4 MN·m, attained at different time instants, are calculated when accounting for the contribution of foundation inertia, with an increase of 34.3 % and 5.4 % for the horizontal load and the moment, respectively. A greater increase is obtained for other systems, reaching a maximum of about 241 % and 10.0 % for Q_{tot} and M_{tot} for a flexible system subjected to a synchronous seismic motion, for which the peak loads

transmitted by the superstructure (Q_s, M_s) are quite low. The point at which the caisson bearing capacity is attained is quite different in the two cases, this corresponding to failure mechanisms characterised by a different depth of the caisson rotation pole [21]. Moreover, the loading path computed accounting for the foundation inertia moves along the interaction domain for some time instants, while this is not observed when considering superstructure inertia only. This results in higher development of permanent displacements during seismic shaking and should be considered for a reliable evaluation of the seismic performance of caisson foundations via simplified numerical approaches such as the rigid-block sliding analysis.

To check the caisson safety against bearing capacity under pseudo-static loading, equivalent horizontal and rotational seismic coefficients $k_{\mathrm{h\ eq}}$ and $k_{\mathrm{rot\ eq}}$ are to be selected, similarly to what done for slopes (e.g.: [34]) the choice mainly depending on the behaviour of the whole soil-foundation-superstructure system. In fact, relying on a ductile system behaviour, equivalent seismic coefficients can be calibrated on desired levels of seismic performance, while peak values of $k_{\mathrm{h\ eq}}$ and $k_{\mathrm{rot\ eq}}$ should be selected for brittle systems. Due to possible second order effects of tall bridge piers with a significant reduction of overall resistance during the seismic event, use of peak values of the seismic coefficients is preferred in this study, neglecting the phase shift between the time histories of $k_{\mathrm{h\ eq}}$ and $k_{\mathrm{rot\ eq}}$, with a consequent safe evaluation of the influence of foundation inertia.

3.1. Equivalent seismic coefficients

The equivalent horizontal and rotational seismic coefficients computed from the 51 dynamic analyses are shown in Figs. 9 and 10. The maximum non-dimensional accelerations at ground surface, $k_{\mathrm{h\ max}}^{(\mathrm{g.s.})} = a_{\mathrm{max}}^{(\mathrm{g.s.})}/g$, are reported in Fig. 9 for comparison; these were computed via 1D free-field response analyses with the Linear-

Equivalent (LE) method ([35], [36]). Values of $k_{h\ eq}$ vary from 0.066 to 0.221; the range of $k_{h\ eq}$ for each seismic input is given in Tab. 4.

Fig. 10 shows the equivalent rotational seismic coefficient $k_{rot\ eq}$ for all the systems and the considered seismic inputs. They range between a minimum of 0.001 and a maximum of 0.012 (Tab. 4).

As expected, higher values of $k_{h\ eq}$ are obtained for squat caissons (embedded shallow foundations) subjected to seismic inputs rich in low frequencies, characterised by high mean periods T_m^{inp} (Tolmezzo, Adana, Dayhook, see Tab. 2) as a result of synchronous motion effects, while the lowest ones are computed for slender caissons (H/D = 2) and seismic inputs rich in high frequencies, that is with low mean periods T_m^{inp} (Assisi, Nocera Umbra, see Tab. 2), where asynchronous motion effects prevail. Conversely, the above kinematic effects result in higher values of $k_{rot\ eq}$ for slender caissons (H/D = 2) and seismic inputs with low T_m^{inp}, whereas lower values are computed for squat caissons (H/D = 0.5) and seismic inputs with high mean periods. However, high values of $k_{h\ eq}$ and $k_{rot\ eq}$ are computed when the ratio between the period of the compliant-base system and that of the soil column in free-field conditions, T_{eq}/T_0, approaches unity, due to dynamic soil-structure coupling, as observed for some piers founded on slender caissons (H/D = 2).

Influence of the Arias intensity of input motions is negligible, as it turned out from the comparison of the values of $k_{h\ eq}$ obtained applying the first set of accelerograms (Tolmezzo, Assisi and Adana) and the second one (Colfiorito, Nocera Umbra and Dayhook), this revealing the role of soil plasticity in limiting the accelerations transmitted to the superstructure in the presence of high-intensity ground motions [17]. As expected, the significant duration of the seismic input does not affect the equivalent seismic coefficients.

4. Empirical relationships

The results discussed in the previous paragraph show that the highest values of the equivalent horizontal seismic coefficient are obtained for squat caissons (low slenderness ratio H/D) subjected to seismic inputs characterised by a high mean period T_m^{inp}, that is when synchronous motion effects prevail in foundation. Conversely, the highest equivalent rotational seismic coefficients are computed for slender caissons (high H/D) subjected to motions with a low mean period T_m^{inp}, that is when asynchronous motion effects are more noticeable. These results can be attributed to the inability of the caisson to follow the deformation imposed by the soil (kinematic effect) and mainly depend on the dimensionless frequency $\beta_0 = 2\pi H/\lambda_m$, that expresses the ratio between the caisson height H and the average wavelength of the seismic motion, λ_m. Moreover, a second aspect can be ascribed to the flexibility of the soil-foundation-superstructure system, that is to its fundamental period T_{eq} (inertial effect). Recently, Gaudio and Rampello [17] showed that the eigenperiod of the whole compliant-base system should be related to the fundamental period of the soil column in free-field conditions, T_0. The accelerations transmitted by the superstructure to the caisson attain their maxima for period ratios $T_{eq}/T_0 \approx 1$, that is close to dynamic coupling between the structure and the soil, and decrease for increasing T_{eq}/T_0. These concepts can be observed in Fig. 11, where the time histories of horizontal acceleration computed close to the head and the base of two caisson foundations are plotted. Fig. 11a refers to a system characterised by the minimum non-dimensional frequency, $\beta_{0,\,min} = 0.22$, computed for a squat caisson (D = 8 m, H/D = 0.5) supporting a bridge pier of height h_s = 30 m subjected to the input of Adana, rich in low frequencies, while Fig. 11b regards the maximum non-dimensional frequency, $\beta_{0,\,max} = 2.92$, obtained for a slender caisson (D = 12 m, H/D = 2) supporting a bridge pier

of height h_s = 30 m subjected to the input of Assisi, rich in high frequencies. In the first case (Fig. 11a) accelerations at the top and at the base of the caisson are always in-phase, this providing a high horizontal seismic coefficient ($k_{h\ eq}$ = 0.164) and an almost null value of the rotational seismic coefficient ($k_{rot\ eq}$ = 0.001). Conversely, in the second case (Fig. 11b), albeit the dynamic coupling between the structure and the soil (T_{eq}/T_0 = 0.93) still yields a high horizontal seismic coefficient ($k_{h\ eq}$ = 0.155), the out-of-phase time histories of horizontal acceleration result in a higher rotational seismic coefficient ($k_{rot\ eq}$ = 0.008).

The equivalent seismic coefficients are then expressed as functions of dimensionless parameters accounting for both kinematic and inertial effects. To this end, the ratio $k_{h\ eq} / k_{h\ max}^{(g.s.)}$ is related to $\gamma_0 = \beta_0 \cdot [T_{eq}/T_0]$ (Fig. 12), while the rotational seismic coefficient $k_{rot\ eq}$ is related to $\delta_0 = \beta_0/[T_{eq}/T_0]$ (Fig. 13). In the evaluation of the non-dimensional frequency β_0, the average wavelength of the seismic motion is computed as $\lambda_m = V_{S,eq} \cdot T_m^{(g.s.)}$, where $V_{S,eq}$ is the equivalent shear wave velocity in the soil interacting with the foundation, extending to a depth $z_{max} = H+2D$, and $T_m^{(g.s.)}$ is the mean period of the seismic motion computed at ground surface, both obtained from 1D, LE response analyses.

Tab. 4 lists the ratios $k_{h\ eq}/k_{h\ max}^{(g.s.)}$ ranging between 0.13 and 0.52 for all the considered seismic inputs. These ratios are a decreasing function of the dimensionless parameter γ_0, as shown in Fig. 12a. Indeed, high values of γ_0 result from high non-dimensional frequencies β_0, that is by asynchronous motions, and from high period ratios T_{eq}/T_0, that is by flexible systems. Under these circumstances, the filtering effect of the embedded foundation [15, 16] contributes to the removal of the high-frequency components of motion, while high period ratios T_{eq}/T_0 correspond to low inertial forces transmitted to

the caisson by the superstructure.

Conversely, the highest values of the ratio $k_{h\ eq}/k_{h\ max}^{(g.s.)}$ are computed for low values of γ_0, that is for a low non-dimensional frequency β_0 and period ratio T_{eq}/T_0, this latter resulting in high forces transmitted by the superstructure to the caisson. For $T_{eq}/T_0 \approx 1$, that is in the presence of dynamic coupling between the structure and the soil, the highest values of the inertial forces are reached, although they are limited by the temporary mobilisation of the soil shear strength during seismic shaking [17]. No remarkable influence of the caisson diameter D has been observed from the results.

The frequency and energy contents of time histories of the horizontal seismic coefficient can shed some light on the above-mentioned kinematic and inertial interaction effects. Fig. 12b shows the ratio between the mean periods of the horizontal seismic coefficient $k_h(t)$ and the seismic motion at ground surface, $T_m^{(h)}/T_m^{(g.s.)}$, as a function of the dimensionless parameter γ_0: it takes values of 0.51 to 1.32, with most of the values lower than unity for $\gamma_0 < 2$ and higher than unity for $\gamma_0 > 2$. As already pointed out, high values of γ_0 are related to asynchronous motions and/or to very flexible systems, the high frequencies being removed and making the mean period to increase. This corresponds to a reduction of the Arias intensity of the time history $k_{h\ eq}(t)$, as shown in Fig. 12c in terms of the ratio $I_A^{(h)}/I_A^{(g.s.)}$, where $I_A^{(g.s.)}$ is the Arias Intensity of the seismic motion at ground surface.

Similar considerations apply to the rotational seismic coefficient $k_{rot\ eq}$, that is an increasing function of $\delta_0 = \beta_0/[T_{eq}/T_0]$ (Fig. 13). In fact, high values of δ_0 are obtained in the presence of asynchronous motions (high β_0) and rigid systems with period ratios T_{eq}/T_0 approaching unity (Fig. 13a). Again, the filtering effect related to kinematic

interaction entails an increase of the mean period of the time history of the rotational seismic coefficient for increasing δ_0 (Fig. 13b) with the ratio $T_m^{(rot)}/T_m^{(g.s.)}$ approaching unity for $\delta_0 > 1.5 \div 2.0$. The Arias intensity of the time history $k_{rot}(t)$ increases with δ_0, reaching the maximum value of $I_A^{(rot)}/I_A^{(g.s.)} \approx 0.02$ % (Fig. 13c). As also discussed for $k_{h\,eq}$, no clear effect of the caisson diameter D is detected for $k_{rot\,eq}$.

To estimate the equivalent seismic coefficients to be used in the safety checks of caisson foundations via a pseudo-static approach, the computed results were best fitted using the following relationships:

$$\frac{k_{h\,eq}}{k_{h\,max}^{(g.s.)}} = B_h \cdot \gamma_0^{A_h} \tag{8}$$

$$k_{rot\,eq} = B_{rot} \cdot e^{A_{rot} \cdot \delta_0} + C_{rot} \tag{9}$$

where the coefficients defining the empirical relationships are listed in Tab. 5, together with their coefficient of determination R^2, this latter given for eq. (8) only as it is the only one falling into the realm of the linear regression models. Although low values of the coefficient of determination R^2 were obtained for eq. (8), it is worth mentioning that an about constant value of $k_{h\,eq}/k_{h\,max}^{(g.s.)} = 0.19$ is calculated for values of $\gamma_0 > 3$. Moreover, a statistically significant (5 %) correlation between the dependent variable $k_{h\,eq}/k_{h\,max}^{(g.s.)}$ and the independent variable γ_0 was detected, as a Student's t-test was performed obtaining very low *p-values*, thus making the null hypothesis of no correlation false (Tab. 5). As far as the rotational seismic coefficient is concerned, a non-linear regression was used to obtain the desired plateau for $\delta_0 \geq 2$. For all the seismic coefficients, the 95 % upper and lower bounds of prediction intervals are plotted as well (see dashed lines in Figs. 12a, Fig. 13a).

The computed empirical relationships are used in the next section, where simple calculation examples are shown and thoroughly discussed.

5. Safety checks against bearing capacity – calculation examples

The inertial forces acting in the caisson foundations can be evaluated using the empirical relationships mentioned above to compute the equivalent horizontal and rotational seismic coefficients, $k_{\mathrm{h\ eq}}$ and $k_{\mathrm{rot\ eq}}$, as a function of the properties of the seismic input and the soil-caisson-superstructure system. The safety check against bearing capacity of caisson foundations subjected to strong seismic events can then be performed following the pseudo-static approach. Two different calculation examples are given, following the prescriptions provided by the Italian Building Code [37].

Calculations are performed for the two systems characterised by caissons of diameter D = 8 and 12 m, both with a slenderness ratio H/D = 1, supporting a 30-m-high bridge pier (see Tab. 3). Following a common procedure adopted in design practice, inertial forces transmitted by the superstructure to the caisson foundations (*superstructure inertia*) are computed performing a linear modal response-spectrum analysis. For both the cases, the design response spectrum is obtained from the results of 1D ground response analyses performed in free-field conditions with the Linear-Equivalent method [35]. In these analyses, the adopted seismic inputs belong to the first set of accelerograms (Tolmezzo, Assisi and Adana, Fig. 3a-b-c). The elastic acceleration spectrum was obtained as the upper-bound envelope of the three acceleration spectra computed at the depth of the caisson centroid, equal to z_G = 4 and 6 m for the caissons with D = 8 and 12 m, respectively, and assuming the spectral shape prescribed by the Italian Building Code [37] (spectra labelled "q = 1" in Fig. 14). The design spectra are obtained reducing

the spectral accelerations by a behaviour factor q = 3.5 (high-class ductility). The peak ground acceleration (Sa at T = 0) is equal to $k_{h\,max}^{(g.s.)}$ = 0.46 and 0.42, respectively. The two systems at hand are modelled in the FE code SAP2000 v.16 [38] through a 3 degrees of freedom lumped-parameter scheme, where the soil compliance is introduced through the translational, rotational and coupled dynamic stiffnesses K_{xx}, K_{rr} and $K_{xr} = K_{rx}$ (the caisson foundations are infinitely rigid, [39]) located at the level of the node representing the foundation, the latter characterised by a mass m_c and a rotational inertia J_c (Fig. 15). The dynamic stiffnesses are evaluated using the well-known relationships proposed by Gazetas [40] at the frequency $f = 1/T_{eq}$, adopting the values of shear modulus G obtained averaging the stiffness profiles provided by the three free-field ground response analyses; values of frequency f were computed following an iterative procedure in which the fundamental frequency was updated until a tolerance smaller than 0.01 was reached. Values of K_{xx}, K_{rr} and K_{xr} obtained at the last step of the iterative procedure are listed in Tab. 6, together with m_c and J_c. It is worth mentioning that, in the linear modal response spectrum analysis, soil contribution to damping cannot be taken into account, unless referring to the complex modal analysis [41], rarely adopted in common practice. The horizontal load Q_s and moment M_s are then multiplied by the over-strength factor γ_{Rd} = 1.3, in the framework of capacity design (Tab. 7a).

Inertial forces acting in the caisson (*foundation inertia*) are determined using eqs. (8) and (9) to evaluate the seismic coefficients $k_{h\,eq}$ and $k_{rot\,eq}$. The non-dimensional frequency β_0 and the period ratio T_{eq}/T_0 are computed as follows:

- $\beta_0 = 2\pi H/\lambda_m$, where $\lambda_m = V_{S,eq} \cdot T_m^{(g.s.)}$. The shear wave velocity $V_{S,eq}$ (Tab. 7a) is calculated as the harmonic average to the depth $z_{max} = H+2D$, thus depending on

the caisson dimensions; $T_m^{(g.s.)}$ = 0.61 s is the average of the mean periods of the three acceleration time histories at ground surface.

- T_{eq} is obtained from the linear modal analyses of the 3 degrees of freedom model performed with the code SAP2000 (Tab. 7a). This resulted in a satisfactory agreement with the values computed using the empirical relationships proposed by Tsigginos *et al*. [27]. Values of T_{eq} = 2.92 and 2.09 s are obtained using SAP2000 for the systems with a caisson of diameter D = 8 and 12 m respectively, while T_{eq} = 2.95 and 2.06 s are evaluated using eq. (1), with a difference smaller than 2 %;
- T_0 = 1.46 s is obtained, as a mean, from the three 1D, LE free-field ground response analyses.

The period ratio T_{eq}/T_0 is then computed in the realm of linear viscous-elasticity, that is accounting for soil plasticity effects in an equivalent manner.

The seismic coefficients computed for the two systems at hand are given in Tab. 7b, while the relevant parameter needed for their computation are listed in Tab. 7a.

Undrained bearing capacity of the two caissons, $R_k = N_{lim,e}$, is evaluated by 3D FE pushover analyses accounting for structure and foundation inertia, Q_{tot} and M_{tot} (eqs. (6) and (7)), amplifying the structure inertial forces by the over-strength factor γ_{Rd} = 1.3. The design value of the caisson bearing capacity, $R_d = R_k/\gamma_R$, is evaluated using the partial factor of safety γ_R = 1.8 prescribed by the Italian Building Code [37]. The design bearing capacity is then compared with the design vertical load acting at the caisson's base $E_d = N_{head} + W_c$. (Tab. 7b).

The safety check against bearing capacity succeeded for both the cases, with ratios of

R_d/E_d equal to 1.15 and 1.04 for caissons with diameter D = 8 m and 12 m, respectively. The higher ratio R_d/E_d is computed for the system with a caisson diameter D = 8 m consistently with its better seismic performance, that is with the lower peak displacements, computed in the dynamic analyses: a drift ratio $u_{rel,\,max}/h_s$ = 3.09 ‰ and 3.40 ‰ was in fact evaluated for the system with D = 8 and 12 m, respectively. This can be ascribed to the higher flexibility of the system with D = 8 m, characterised by a period ratio T_{eq}/T_0 = 2.00, this resulting in smaller forces transmitted to the foundation, compared to those obtained for the system with D = 12 m, that is stiffer (T_{eq}/T_0 = 1.43). The horizontal force associated to foundation inertia, $k_{h\,eq}\cdot W_c$, is not negligible in both cases in that it is equal to 48 % of the total design horizontal force $Q_{tot,\,d} = Q_s\cdot \gamma_{Rd} + \Delta Q$ for D = 8 m and to about 34 % for the system with D = 12 m, while a negligible influence of the foundation inertia is obtained for the moment M_{tot} (1.0 and 1.5 % for D = 8 m and 12 m).

6. Conclusions

Safety assessment against bearing capacity of caisson foundations subjected to strong ground motions using the pseudo-static approach requires a proper evaluation of the inertial forces acting in the structure and the foundation, the latter being not negligible for massive foundations.

In this paper, the influence of the inertial forces acting in the caisson foundations of bridge piers is evaluated using the results of a parametric study where 14 different soil-caisson-pier-deck systems were subjected to 6 real high-intensity ground motions via 51 non-linear 3D FE dynamic analyses [17]. All systems were designed to deliver a given initial safety factor against bearing capacity, in order to fairly compare the analysis results.

A substantial influence of foundation inertia on the horizontal force is detected with possible maximum increases of about 240 % with respect to the horizontal load transmitted by the superstructure only, while a smaller increase of about 10 % is obtained for the rotational inertia acting in the caisson.

Considering foundation inertia, caisson bearing capacity is reached at a different point in the interaction domain with respect to that calculated ignoring it, foundation inertia being responsible for a greater accumulation of permanent caisson displacements during the seismic event, as it can make the load path move along the interaction domain for more than just a time instant.

Hence, inertial forces acting in fully embedded massive foundations should be accounted for when developing simplified models for evaluating their seismic performance (e.g.: Newmark type analyses) or when calibrating macro-element models for caisson foundations.

The equivalent horizontal and rotational seismic coefficients $k_{\mathrm{h\,eq}}$ an $k_{\mathrm{rot\,eq}}$, to be used in a pseudo-static approach, have been assumed as the peak values of the time histories of the inertial forces acting in the caissons, as obtained from the dynamic analyses of the parametric study. The horizontal seismic coefficient $k_{\mathrm{h\,eq}}$ is always lower than the maximum value attained at ground surface in free-field conditions, $k_{\mathrm{h\,max}}^{(\mathrm{g.s.})}$, with a decrease of 48 to 87 %. Both the seismic coefficients depend on kinematic and inertial interaction effects, the former mainly ruled by the non-dimensional frequency β_0, while the latter by the period ratio T_{eq}/T_0. The more the period ratio T_{eq}/T_0 is close to unity, the higher are both $k_{\mathrm{h\,eq}}$ an $k_{\mathrm{rot\,eq}}$. Moreover, greater values of $k_{\mathrm{h\,eq}}$ are obtained for squat caissons subjected to seismic inputs rich in low frequencies, this corresponding to

synchronous motion with a low non-dimensional frequency, whereas higher values of $k_{\mathrm{rot\ eq}}$ are computed for slender caissons subjected to ground motions rich in high frequency components, that is to asynchronous motion with high values of β_0.

Physically sound empirical relationships are proposed to estimate the equivalent seismic coefficients, these requiring the dimensionless parameters $\gamma_0 = \beta_0 \cdot [T_{\mathrm{eq}}/T_0]$ and $\delta_0 = \beta_0/[T_{\mathrm{eq}}/T_0]$ to be computed.

Two calculation examples of caisson safety against bearing capacity are shown using the pseudo-static approach, where the major role of the horizontal seismic coefficient $k_{\mathrm{h\ eq}}$ than that of the rotational coefficient $k_{\mathrm{rot\ eq}}$ is demonstrated. More importantly, using the seismic coefficients provided by the proposed empirical relationships, the pseudo-static approach provides results consistent with the ones obtained from the dynamic analyses, in that the higher safety factor is computed for the system for which a better seismic performance is computed by the dynamic analyses, while the lower safety factor is obtained for the system that suffers the greater earthquake-induced displacements.

Further developments of the study would require a larger seismic database to be adopted and the calibration of the seismic coefficients against desired levels of seismic performance, typically expressed in terms of maximum and permanent displacements induced by seismic loading. However, assuming the equivalent seismic coefficients equal to the peak values of the time histories of inertial forces acting in the caisson yields to a safe assessment of bearing capacity, including systems that may suffer a brittle seismic performance due to second order effects.

Acknowledgements

The Authors would like to sincerely thank Prof. L. Callisto for his useful comments and suggestions. Part of this research was funded by the Department of Civil Protection through the ReLUIS (University Network of Seismic Engineering Laboratories) Consortium.

1 List of symbols

$a_c\,(t)$	horizontal acceleration time history acting in the caisson
$a_{ff}\,(t)$	horizontal acceleration time history acting in the soil in free-field conditions
$a_{max}^{(g.s.)}$	maximum acceleration at ground surface in free-field conditions
a_{max}^{inp}	peak horizontal acceleration of input motion
c'	effective cohesion
D	caisson diameter
E	soil Young's modulus
E_{50}^{ref}	soil secant modulus at 50% of strength at the reference pressure p_{ref} = 100 kPa
E_c	caisson Young's modulus
E_{oed}^{ref}	tangent stiffness for primary oedometer loading at the reference pressure p_{ref} = 100 kPa
E_{ur}^{ref}	unloading-reloading Young's modulus at the reference pressure p_{ref} = 100 kPa
F_{Se}	safety factors against bearing capacity under pseudo-static conditions
F_{Sv}	safety factors against bearing capacity under static conditions
G_0	small-strain shear modulus
G_0^{ref}	small-strain shear modulus at the reference pressure p_{ref} = 100 kPa
G_s	secant shear modulus
H	caisson height
h_s	pier height
$I_A^{(g.s.)}$	Arias Intensity of seismic motion at ground surface in free-field conditions
$I_A^{(h)}$	Arias Intensity of $k_h(t)$
$I_A^{(rot)}$	Arias Intensity of $k_{rot}(t)$
I_A^{inp}	Arias intensity of input motion
J_c	rotational inertia of the caisson
$k_h\,(t)$	time history of the horizontal seismic coefficient
$k_{h\,eq}$	equivalent horizontal seismic coefficient
$k_{h\,max}^{(g.s.)}$	maximum seismic coefficient at the ground surface in free-field conditions
$k_{rot}\,(t)$	time history of the rotational seismic coefficient
$k_{rot\,eq}$	equivalent rotational seismic coefficient
K_{rr}	rotational dynamic stiffness of the soil-caisson system
k_s	flexural stiffness of the pier
$k_{v\,eq}$	equivalent vertical seismic coefficient

$K_{xr} = K_{rx}$	coupled dynamic stiffness of the soil-caisson system
K_{xx}	translational dynamic stiffness of the soil-caisson system
m	dimensionless stiffness parameter
m_c	caisson mass
$M_c\,(t)$	time history of the moment acting in the caisson
m_{deck}	deck mass
m_{ff}	soil mass
$M_{ff}\,(t)$	time history of the moment acting in the soil in free-field conditions
m_{pier}	pier mass
$M_s\,(t)$	time history of the bending moment at the base of the pier
m_s	lumped mass of the Single Degree of Freedom system representing the superstructure
$M_{tot}\,(t)$	time history of the total moment acting at the top of the caisson
N_{head}	vertical load at the top of the caisson
$N_{head,lim}$	vertical load at the top of the caisson bringing the foundation to limit conditions
$N_{lim,e}$	bearing capacity of the caisson foundation under pseudo-static conditions
OCR	overconsolidation ratio
q	behaviour factor
$Q_c\,(t)$	time history of the horizontal force acting in the caisson
$Q_{ff}\,(t)$	time history of the horizontal force acting in the soil in free-field conditions
$Q_{lim,e}$	limit sliding force at the base of the caisson under pseudo-static conditions
$Q_s\,(t)$	time history of the horizontal force at the base of the pier
$Q_{tot,\,d}$	design value of the total horizontal force acting at the top of the caisson
$Q_{tot}\,(t)$	time history of the total horizontal force acting at the top of the caisson
Sa	spectral acceleration
T_0	fundamental period of the soil in free-field conditions
T_D^{inp}	significant duration of the input motion
T_{eq}	equivalent fundamental period
$T_m^{(g.s.)}$	mean period of seismic motion at ground surface in free-field conditions
T_m^{inp}	mean period of input motion
$T_m^{(h)}$	mean period of $k_h(t)$
$T_m^{(rot)}$	mean period of $k_{rot}(t)$

T_R	return period
T_s	fundamental period of the fixed-base pier
u_{rel}	horizontal drift between deck and caisson
V_N	design working life
$V_{S,eq} = \dfrac{H+2D}{\sum_{i=1}^{n} \dfrac{h_i}{V_{S,i}}}$	equivalent shear wave velocity of the soil interacting with the foundation
W_c	caisson weight
$z_G = H/2$	depth of caisson centroid
β_0	dimensionless frequency
γ	soil unit weight
$\gamma_0 = \beta_0 \cdot [T_{eq}/T_0]$	dimensionless parameter affecting $k_{h\ eq}$
$\gamma_{0.7}$	shear strain corresponding to a decay of secant shear modulus $G_s/G_0 = 0.722$
γ_R	partial factor of safety
γ_{Rd}	over-strength factor
$\delta_0 = \beta_0/[T_{eq}/T_0]$	dimensionless parameter affecting $k_{rot\ eq}$
$\ddot{\theta}_c(t)$	time history of the angular acceleration of the caisson
λ_m	average wavelength of the seismic motion
ν_{ur}	Poisson's ratio
ξ_s	damping ratio of the pier
ρ	soil density
ρ_c	caisson density
$\sigma_{z\ (0.5pier)}$	vertical stress representing the lower half of the pier
φ'	angle of shearing resistance

1

References

[1] Paolucci R. Simplified evaluation of earthquake-induced permanent displacement of shallow foundations. J Earth Eng 1997; 1(3): 563-79.

[2] Paolucci R, Shirato M, Yilmaz MT. Seismic behaviour of shallow foundations: Shaking table experiments vs numerical modelling. Earth Eng Struc Dyn 2008; 37(4): 577-95.

[3] Chatzigogos CT, Pecker A, Salençon J. Macroelement modeling of shallow foundations. Soil Dyn Earth Eng 2009; 29: 765-81.

[4] Chatzigogos CT, Pecker A, Salençon J. Displacement-based design of shallow foundations with macroelement. Soils Found 2009; 49(6): 853-69.

[5] Pisanò F, di Prisco CG, Lancellotta R. Soil–foundation modelling in laterally loaded historical towers. Géotechnique 2014; 64(1):1–15.

[6] Pisanò F, Flessati L, di Prisco CG. A macroelement framework for shallow foundations including changes in configuration. Géotechnique 2016; 66(11):910–26.

[7] Richards Jr R, Elms DG, Budhu M. Seismic bearing capacity and settlements of foundations. J Geotech Eng, ASCE 1993; 119(4): 662-74.

[8] Paolucci R, Pecker A. Seismic bearing capacity of shallow strip foundations on dry soils. Soils Found 1997; 37(3): 95-105.

[9] Paolucci R, Pecker A. Soil inertia effects on the bearing capacity of rectangular foundations on cohesive soils. Eng Struct 1997; 19(8):637-43.

[10] Cascone E, Casablanca O. Static and seismic bearing capacity of shallow strip footings. Soil Dyn Earthq Eng 2016; 84:204–23.

[11] Pane V, Vecchietti A, Cecconi M. A numerical study on the seismic bearing capacity of shallow foundations. Bull Earthq Eng 2016;14(11):2931–58.

[12] Conti R. Simplified formulas for the seismic bearing capacity of shallow strip foundations. Soil Dyn Earthq Eng 2018; 104, 64-74.

[13] Izumi Y, Miura K. The design seismic coefficient of the embedding foundation on building structures. Proceedings on 12th World Conference on Earthquake Engineering, Vancouver, Canada; 2004. p. 1-9.

[14] Gerolymos N, Gazetas G. Winkler model for lateral response of rigid caisson foundations in linear soil. Soil Dyn Earthq Eng 2006; 26(5), 347-61.

[15] Conti R, Morigi M, Viggiani GMB. Filtering effect induced by rigid massless embedded foundations. Bull Earthq Eng 2017; 15(3):1019–35.

[16] Conti R, Morigi M, Rovithis E, Theodoulidis N, Karakostas C. Filtering action of embedded massive foundations: New analytical expressions and evidence from 2 instrumented buildings. Earthq Eng Struct Dyn 2018; 47(5):1229–49.

[17] Gaudio D, Rampello S. The influence of soil plasticity on the seismic performance of bridge piers on caisson foundations. Soil Dynamics and Earthquake Engineering, 2019; 118, 120-33. DOI: 10.1016/j.soildyn.2018.12.007

[18] Gaudio D, Rampello S. The role of soil constitutive modelling on the assessment of seismic performance of caisson foundations. In: Proceedings of the 7th International Conference on Earthquake Geotechnical Engineering, Rome, Italy; 2019:2574-2582.

[19] Gaudio D. Interazione dinamica terreno-struttura di pozzi di fondazione di pile di ponti e viadotti [Ph.D. thesis, in Italian]. Rome, Italy: Sapienza University of Rome; 2017

⟨https://iris.uniroma1.it/handle/11573/947638?mode=full.365#.WQb1QPnyiUk⟩.

[20] Zafeirakos A, Gerolymos N. Towards a seismic capacity design of caisson foundations supporting bridge piers. Soil Dyn Earthq Eng 2014; 67:179–97.

[21] Gerolymos N, Zafeirakos A, Karapiperis K. Generalized failure envelope for caisson foundations in cohesive soil: Static and dynamic loading. Soil Dyn Earthq Eng 2015; 78:154–74.

[22] Benz T, Vermeer PA, Schwab R. A small-strain overlay model. Int J Numer Anal Methods Geomech 2009; 33(1):25–44.

[23] Brinkgreve RBJ, Engine E, Swolfs WM. PLAXIS 3D. Reference Manual; 2013.

[24] Arias A. A measure of earthquake intensity. Seismic design for nuclear power plants. Cambridge, MA: Massachusetts Institute of Technology Press; 1970. p. 438–83.

[25] Rathje EM, Abrahamson NA, Bray JD. Simplified frequency content estimates of earthquake ground motions. J Geotech Geoenviron Eng 1998;124(2):150–9.

[26] Trifunac MD, Brady AG. A study on the duration of strong earthquake ground motion. Bull Seismol Soc Am 1975;65(3):581–626.

[27] Tsigginos C, Gerolymos N, Assimaki D, Gazetas G. Seismic response of bridge pier on rigid caisson in soil stratum. Earthq Eng Eng Vib 2008;7(1):33–44.

[28] Gaudio D, Rampello S. A simplified procedure for the evaluation of the seismic performance of bridge piers on caisson foundations. In: Proceedings of COMPDYN 2019 - 7th ECCOMAS Thematic Conference on Computational Methods in Structural Dynamics and Earthquake Engineering M. Papadrakakis, M. Fragiadakis (eds.), Crete, Greece; 24–26 June 2019: 1-11 ⟨https://2019.compdyn.org/proceedings/pdf/19755.pdf⟩

[29] Zafeirakos A, Gerolymos N. On the seismic response of under-designed caisson foundations, Bull Earthq Eng 2013;11(5):1337–72.

[30] Brinch Hansen J. A revised and extended formula for bearing capacity. Copenhagen: Bulletin No. 28 of Danish Geotechnical Institute; 1970.

[31] Froelich X. Beitrag fur Berechnung von Mastfundamenten. Ernest, Berlin; 1936.

[32] Gaudio D, Rampello S. Dynamic soil-structure interaction of bridge-pier caisson foundations. In Geotechnical engineering in multidisciplinary research: from microscale to regional scale CNRIG2016. In: Proceedings of the VI Italian conference of researchers in geotechnical engineering, procedia engineering 158, 2016. p. 146–151. DOI: 10.1016/j.proeng.2016.08.420

[33] Zafeirakos A, Gerolymos N. Bearing strength surface for bridge caisson foundations in frictional soil under combined loading. Acta Geotech 2016;11(5):1189–208.

[34] Seed HB, Martin GR. The seismic coefficient on earth dam design. J Soil Mech Found Div, ASCE 1966; 92(3): 25-58.

[35] Idriss IM, Seed HM. Response of horizontal soil layers during earthquakes. J Soil Mech Found Div, ASCE 1968; SM4: 1003-31.

[36] Callisto L. MARTA v. 1.1: a computer program for the site response analysis of a layered deposit. http://luigicallisto.site.uniroma1.it/attivita-1.; 2015.

[37] Ministero delle Infrastrutture. Norme tecniche per le Costruzioni. Gazzetta Ufficiale della Repubblica Italiana 42, Decreto Ministero Infrastrutture 17.01.2018, Rome (in Italian); 2018.

[38] CSI (Computer and Structures Inc.). SAP2000: integrated finite element analysis and design of structures. Berkeley, California; 2013.

[39] Varun, Assimaki D, Gazetas G. A simplified model for lateral response of large diameter caisson foundations - Linear elastic formulation. Soil Dyn Earthq Eng 2009; 29(2):268–91.

[40] Gazetas G. Foundation vibrations. In: Springer US ed. Foundation engineering handbook, 1991: 553-93.

[41] Veletsos AS, Ventura CE. Modal analysis of non-classically damped linear systems. Earth Eng Struct Dyn 1986; 14(2): 217-43.

Tables

Table 1. Parameters assumed for the foundation soils

soil	γ (kN/m^3)	c' (kPa)	φ' (°)	OCR (-)	k_0 (-)	G_0^{ref} (MPa)	m (-)	$\gamma_{0.7}$ (%)	E'_{ur}^{ref} (MPa)
gravelly sand	20	0	30	10	0.5	145.7	0.61	0.024	174.9
silty clay	20	20	23	4.4÷1.5	1.1÷0.7	65.7	0.75	0.045	58.2

Table 2. Synthetic ground motion parameters of selected scaled seismic inputs

record	F (-)	a_{max}^{inp} (g)	I_A^{inp} (m/s)	T_m^{inp} (s)	T_D^{inp} (s)
Tolmezzo E-W (1978)	1.00	0.316	1.17	0.50	5.220
Assisi E-W (1997)	2.00	0.332	1.12	0.24	4.295
Adana E-W (1998)	1.05	0.292	1.17	0.62	12.990
Colfiorito N-S (1997)	2.00	0.676	2.79	0.51	5.115
Nocera Umbra N-S (1997)	1.00	0.502	2.87	0.21	4.640
Dayhook N-S (1978)	1.45	0.573	2.84	0.46	12.870

Table 3. Geometric and mechanical properties of the systems considered in the parametric study

D (m)	H/D (-)	h_s (m)	k_s (MN/m)	m_s (Mg)	T_{eq} (s)
8	0.5	30	10.1	1376.4	3.22
	1	30	11.8	1608.9	2.95
		60	6.2	1208.1	3.59
	2	15	102.4	2171.4	1.26
		30	46.9	2016.1	1.80
		60	20.8	1694.9	2.47
12	0.5	15	106.4	3501.7	1.76
		30	37.7	3365.9	2.76
		60	19.8	2858.6	3.62
	1	15	169.3	4227.8	1.43
		30	78.7	4050.6	2.06
		60	29.9	3568.1	3.05
	2	30	411.2	5439.0	1.26
		60	192.3	4132.7	1.61

Table 4. Minimum and maximum values of the equivalent seismic coefficients and ratio between the equivalent horizontal and the maximum seismic coefficient computed at the ground surface level in free-field conditions

record	$k_{h\ eq}$ (1)	$k_{h\ max}^{(g.s.)}$ (2)	(1)/(2)	$k_{rot\ eq}$
Tolmezzo	0.079÷0.221	0.491	0.16÷0.45	0.002÷0.010
Assisi	0.066÷0.156	0.491	0.13÷0.32	0.002÷0.012
Adana	0.080÷0.164	0.486	0.17÷0.34	0.001÷0.010
Colfiorito	0.091÷0.149	0.602	0.15÷0.25	0.003÷0.009
Nocera Umbra	0.083÷0.201	0.391	0.21÷0.52	0.004÷0.010
Dayhook	0.091÷0.216	0.640	0.14÷0.34	0.003÷0.008

Table 5. Coefficients of the empirical relationships defined in eqs. (8) and (9)

eq. (8)				eq. (9)		
A_h	B_h	R^2	*p-value*	A_{rot}	B_{rot}	C_{rot}
-0.1984	0.2371	0.1584	0.0038	-2.139	-0.0101	0.0093

Table 6. Dynamic stiffnesses and inertial properties of the caisson foundations considered in the calculation examples

D (m)	m_c (Mg)	J_c (Mg·m^2)	K_{xx} (GN/m)	$K_{xr} = K_{rx}$ (GN·m/m)	K_{rr} (GN·m)
8	1024.8	9564.6	2.36	-3.25	29.9
12	3458.6	72631.3	4.54	-9.25	119.6

Table 7a. Loads transmitted by the superstructure to the caissons and dimensionless parameters adopted for the evaluation of inertial forces acting in the foundations

D (m)	N_{head} (MN)	$Q_s \cdot \gamma_{Rd}$ (MN)	$M_s \cdot \gamma_{Rd}$ (MN·m)	$V_{S,\ eq}$ (m/s)	β_0 (-)	T_{eq}/T_0 (s)	γ_0 (-)	δ_0 (-)
8	16.85	1.14	34.24	139.8	0.59	2.00	1.18	0.30
12	42.14	6.40	192.12	147.5	0.84	1.43	1.20	0.59

Table 7b. Inertial forces computed using eqs. (8) and (9) and safety checks against bearing capacity

$k_{h\ eq}/k_{h\ max}^{(g.s.)}$ (-)	$k_{h\ max}^{(g.s.)}$ (-)	$k_{h\ eq}$ (-)	$k_{rot\ eq}$ (-)	W_c (MN)	$k_{h\ eq} \cdot W_c$ (MN)	$k_{rot\ eq} \cdot W_c \cdot D$ (MN·m)	E_d (MN)	R_d (MN)	R_d/E_d (-)
0.23	0.46	0.105	0.004	10.05	1.05	0.32	26.90	31.10	1.15
0.23	0.42	0.097	0.006	33.93	3.28	2.61	76.06	79.24	1.04

Figure captions

Fig. 1. Schematic layout of forces acting on a caisson foundation reaching its bearing capacity under earthquake loading. Forces and stresses acting outside of the plane are not shown for the sake of clarity.

Fig. 2. (a) Schematic layout of the problem; (b) overconsolidation ratio and small-strain shear modulus profiles assumed in the analyses; (c) three-dimensional finite element model adopted in the parametric study.

Fig. 3. Scaled seismic input motions: (a) and (d) acceleration time histories; (b) and (e) Arias intensity time histories; (c) and (f) Fourier amplitude spectra.

Fig. 4. Layout adopted for the calculation of the horizontal and rotational seismic coefficients.

Fig. 5. Horizontal acceleration profiles: (a) into the caisson and (b) in the soil column under free-field conditions, computed at some time instants (I_A^{inp} = 5, 70, 90 and 99 %) for D = 12 m, H/D = 2, h_s = 30 m, Adana record.

Fig. 6 Calculation of the seismic coefficients at t = 11.705 s, for D = 12 m, H/D = 2, h_s = 30 m, Adana record. Profiles of the: (a) horizontal acceleration into the caisson and in the 1D soil column; (b) weighted difference between the caisson and the free-field horizontal accelerations; (c) caisson angular acceleration.

Fig. 7. Time histories of seismic coefficients for D = 12 m, H/D = 2, h_s = 30 m, Adana record: (a) horizontal seismic coefficient; (b) rotational seismic coefficient.

Fig. 8. Load paths at the top of the caisson with and without considering foundation inertia (D = 12 m, H/D = 2, h_s = 30 m, Adana record).

Fig. 9. Equivalent horizontal seismic coefficient computed in the 51 dynamic analyses.

Fig. 10. Equivalent rotational seismic coefficient computed in the 51 dynamic analyses.

Fig. 11. Horizontal acceleration time histories computed into the caisson for the (a) minimum and (b) maximum value of the dimensionless frequency β_0.

Fig. 12. Ratio of: (a) the equivalent horizontal seismic coefficient to the peak horizontal seismic coefficient computed at the ground surface through the Linear-Equivalent Method [35], (b) mean period and (c) Arias intensity of the horizontal seismic coefficient time histories to the ones of the seismic motion computed at the ground surface in free-field conditions.

Fig. 13. (a) Equivalent rotational seismic coefficient. Ratio between the (b) mean period and (c) Arias intensity of the rotational seismic coefficient time histories to the ones of the seismic motion computed at the ground surface in free-field conditions.

Fig. 14. Elastic acceleration spectra for the piers with h_s = 30 m supported by caissons with slenderness ratio H/D = 1 and (a) D = 8 m; (b) D = 12 m, adopting the first set of input motions.

Fig. 15. Kinematics of the 3 degrees of freedom systems modelled in the FE code SAP2000 v.16 [38].

Figures

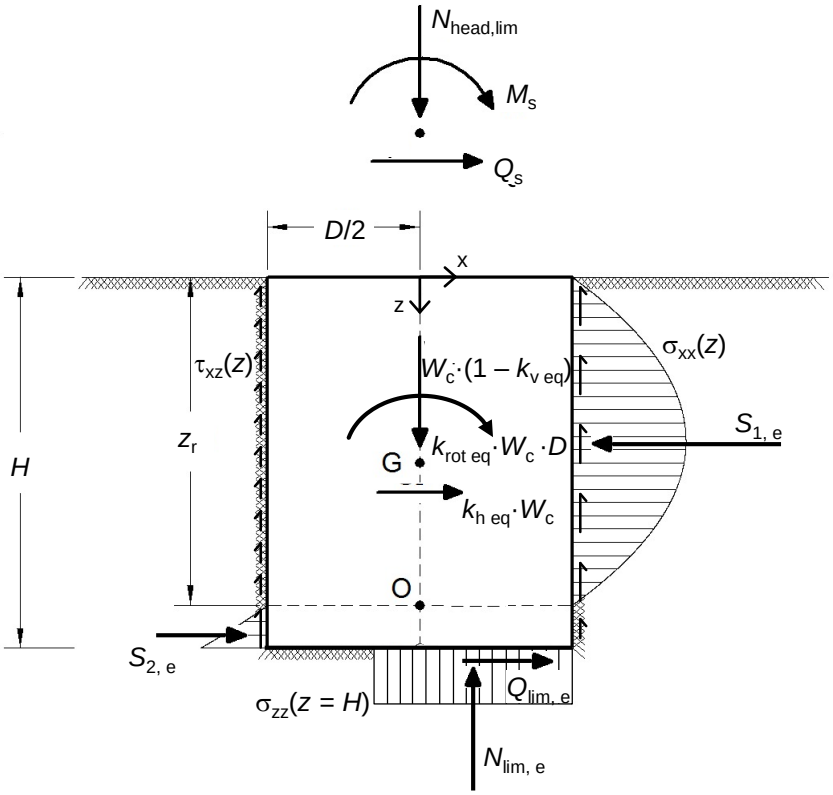

Fig. 1. Schematic layout of forces acting on a caisson foundation reaching its bearing capacity under earthquake loading. Forces and stresses acting outside of the plane are not shown for the sake of clarity.

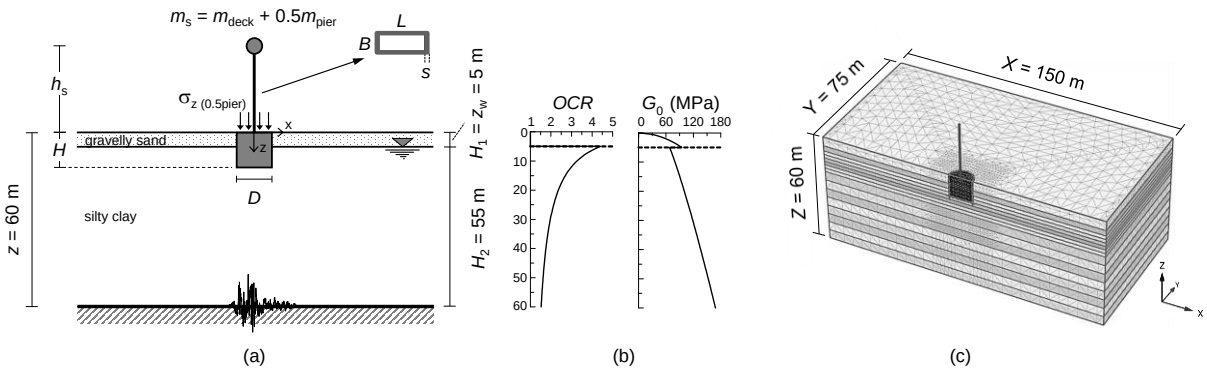

Fig. 2. (a) Schematic layout of the problem; (b) overconsolidation ratio and small-strain shear modulus profiles assumed in the analyses; (c) three-dimensional finite element model adopted in the parametric study.

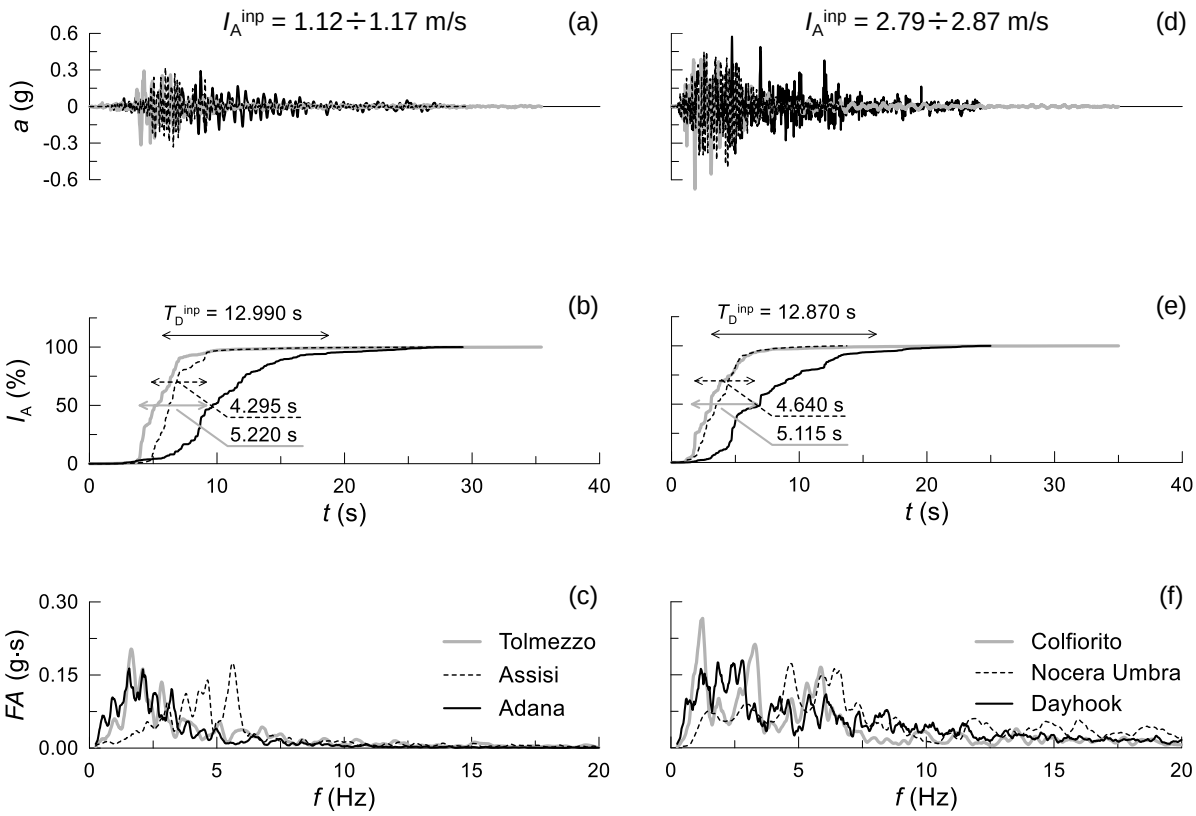

Fig. 3. Scaled seismic input motions: (a) and (d) acceleration time histories; (b) and (e) Arias intensity time histories; (c) and (f) Fourier amplitude spectra.

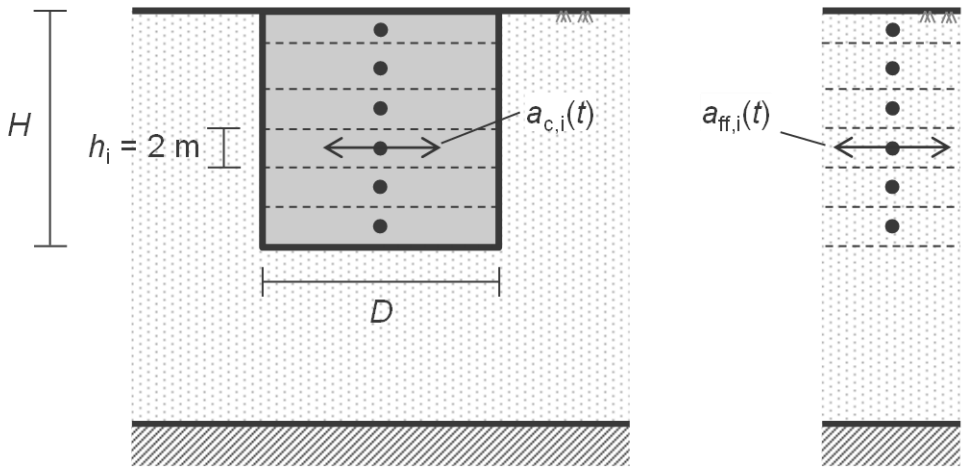

Fig. 4. Layout adopted for the calculation of the horizontal and rotational seismic coefficients.

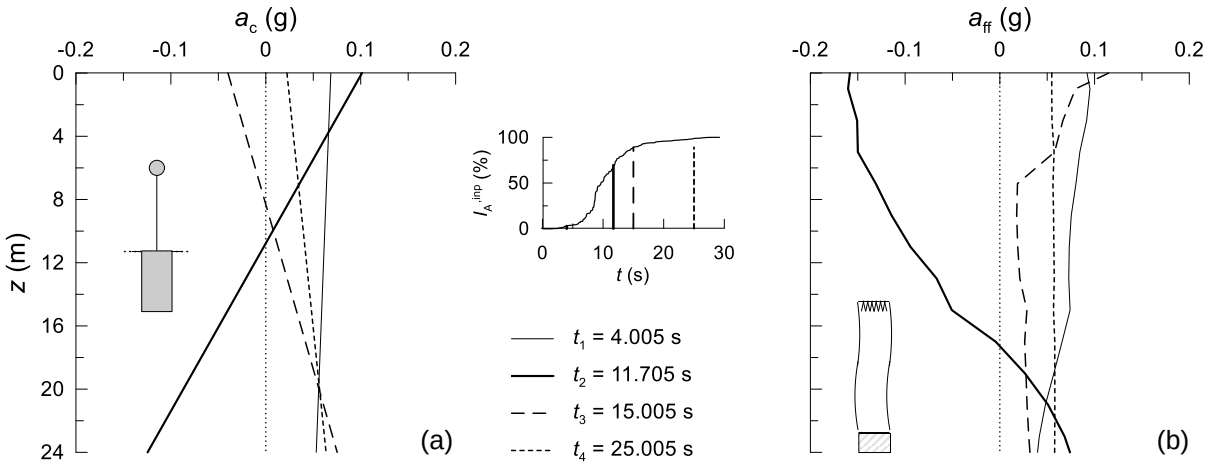

Fig. 5. Horizontal acceleration profiles: (a) into the caisson and (b) in the soil column under free-field conditions, computed at some time instants (I_A^{inp} = 5, 70, 90 and 99 %) for D = 12 m, H/D = 2, h_s = 30 m, Adana record.

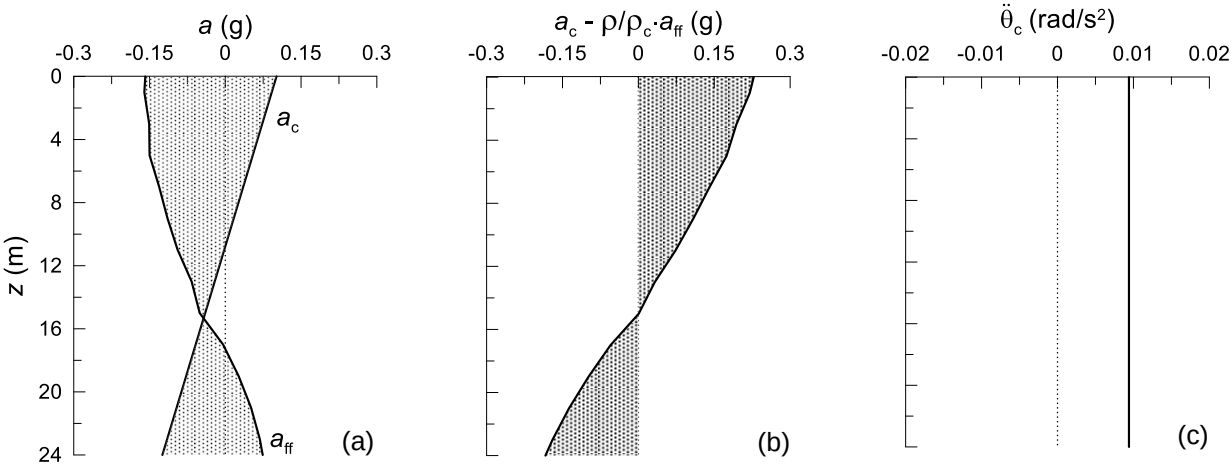

Fig. 6. Calculation of the seismic coefficients at t = 11.705 s, for D = 12 m, H/D = 2, h_s = 30 m, Adana record. Profiles of the: (a) horizontal acceleration into the caisson and in the 1D soil column; (b) weighted difference between the caisson and the free-field horizontal accelerations; (c) caisson angular acceleration.

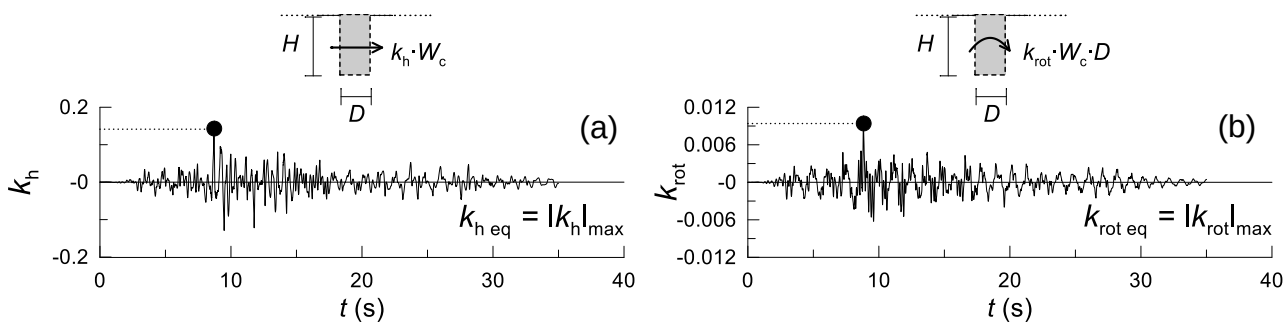

Fig. 7. Time histories of seismic coefficients for D = 12 m, H/D = 2, h_s = 30 m, Adana record: (a) horizontal seismic coefficient; (b) rotational seismic coefficient.

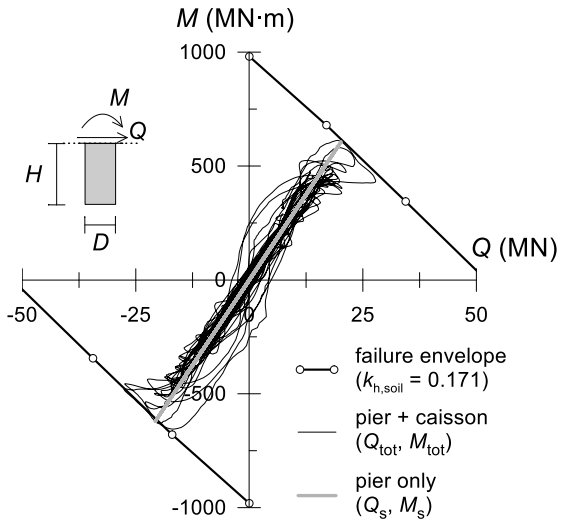

Fig. 8. Load paths at the top of the caisson with and without considering foundation inertia (D = 12 m, H/D = 2, h_s = 30 m, Adana record).

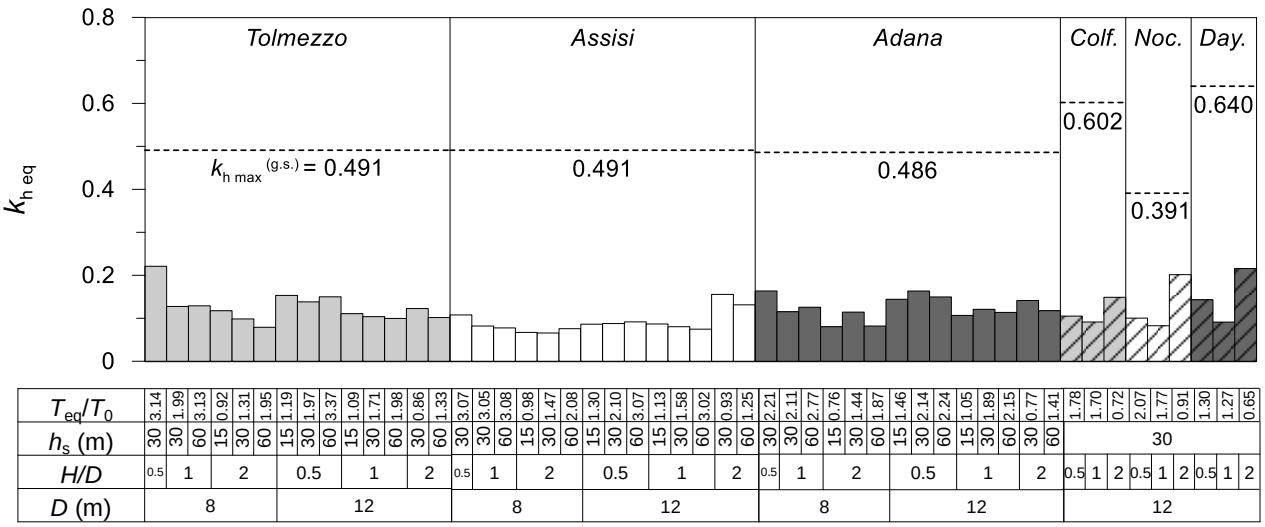

Fig. 9. Equivalent horizontal seismic coefficient computed in the 51 dynamic analyses.

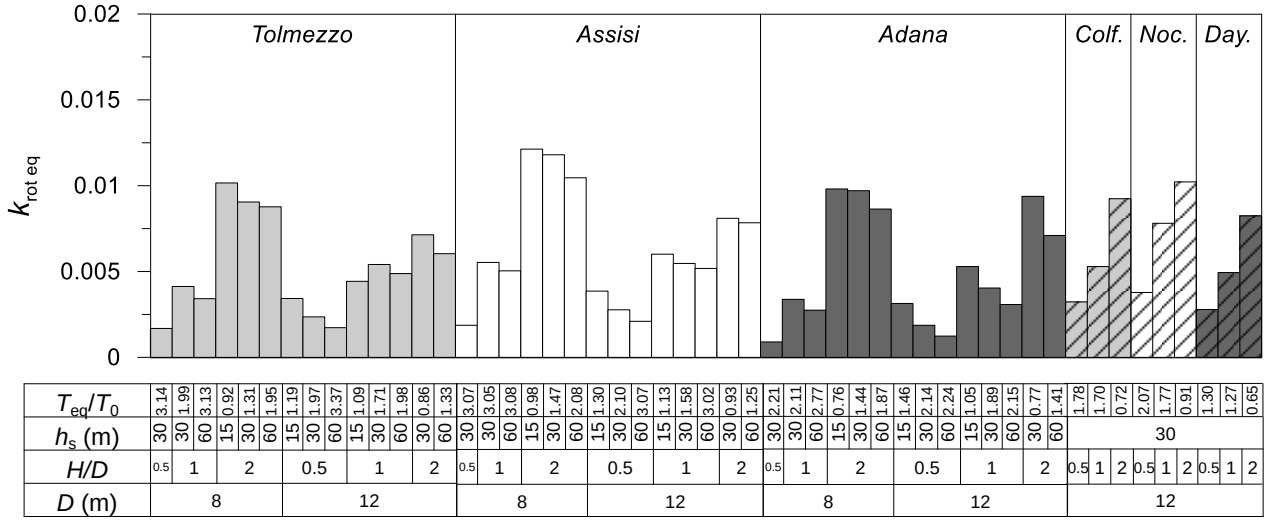

Fig. 10. Equivalent rotational seismic coefficient computed in the 51 dynamic analyses.

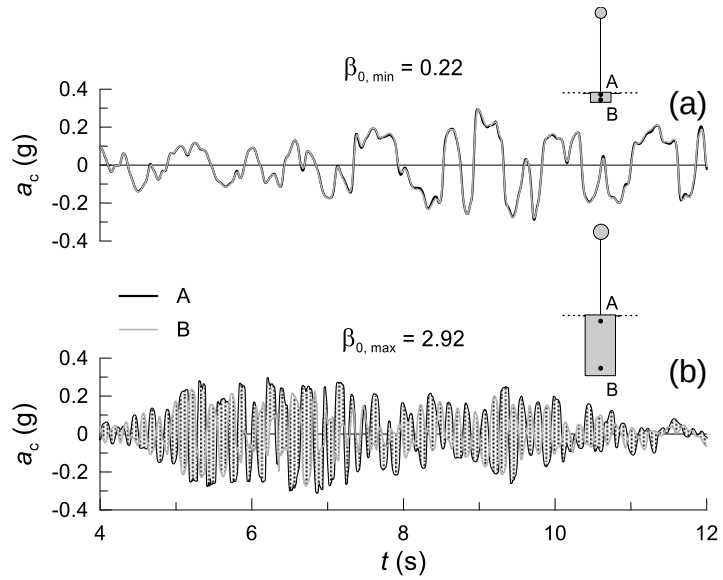

Fig. 11. Horizontal acceleration time histories computed into the caisson for the (a) minimum and (b) maximum value of the dimensionless frequency β_0.

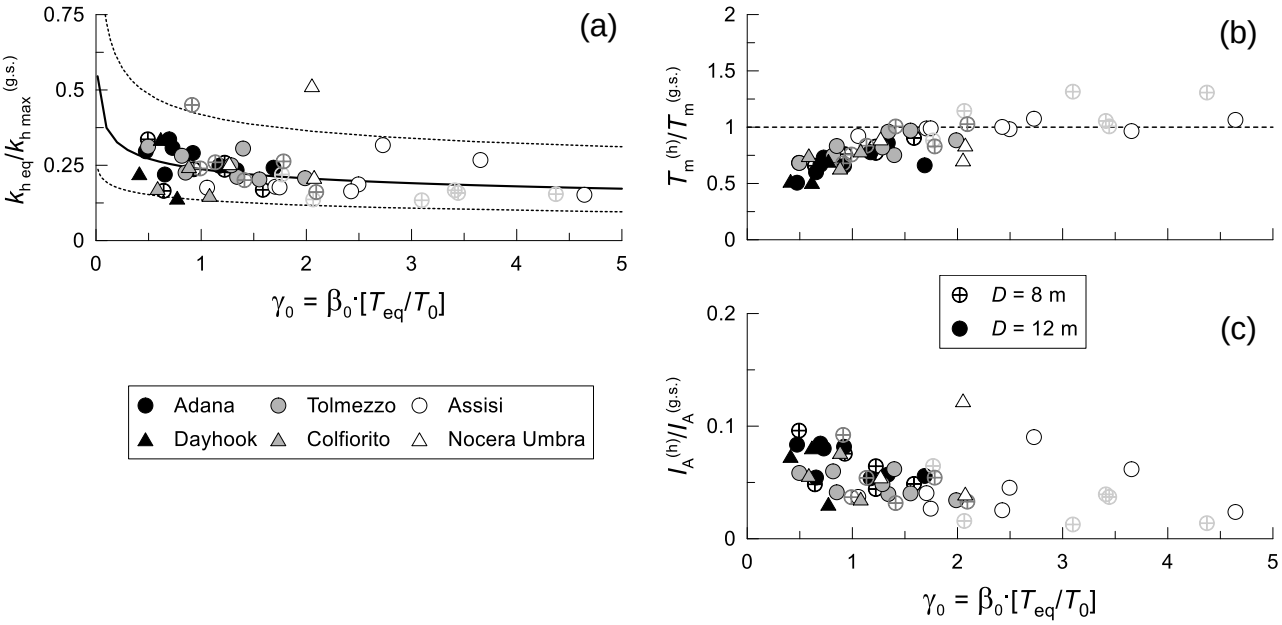

Fig. 12. Ratio of: (a) the equivalent horizontal seismic coefficient to the peak horizontal seismic coefficient computed at the ground surface through the Linear-Equivalent Method [35], (b) mean period and (c) Arias intensity of the horizontal seismic coefficient time histories to the ones of the seismic motion computed at the ground surface in free-field conditions.

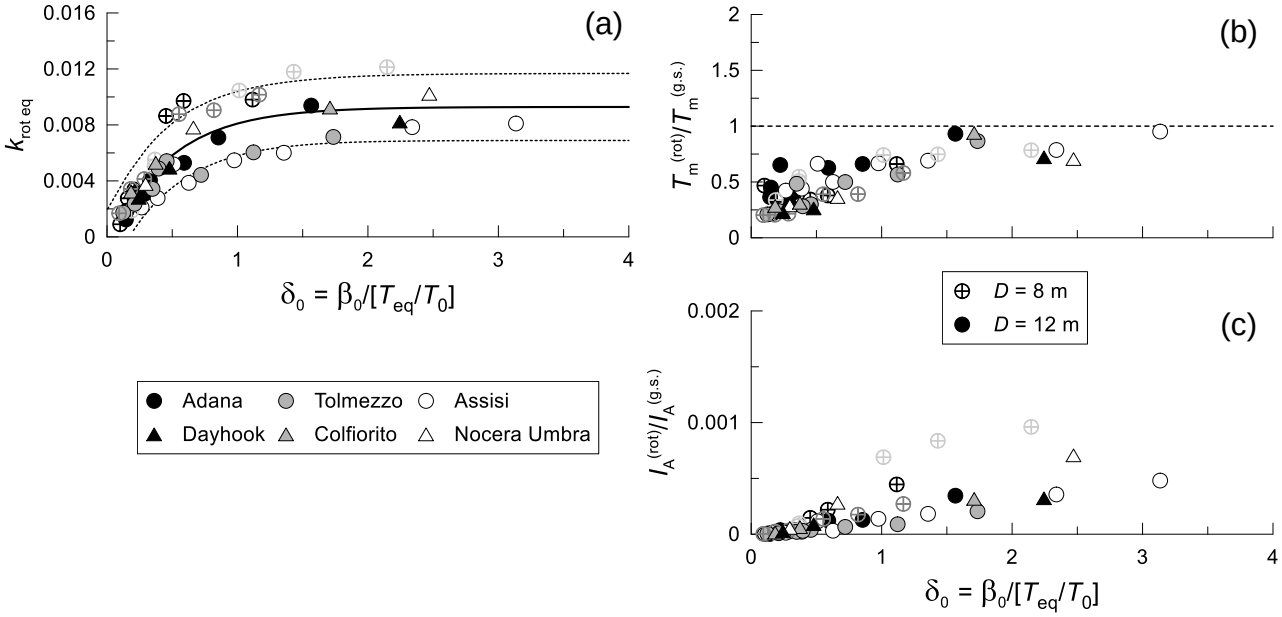

Fig. 13. (a) Equivalent rotational seismic coefficient. Ratio between the (b) mean period and (c) Arias intensity of the rotational seismic coefficient time histories to the ones of the input motion.

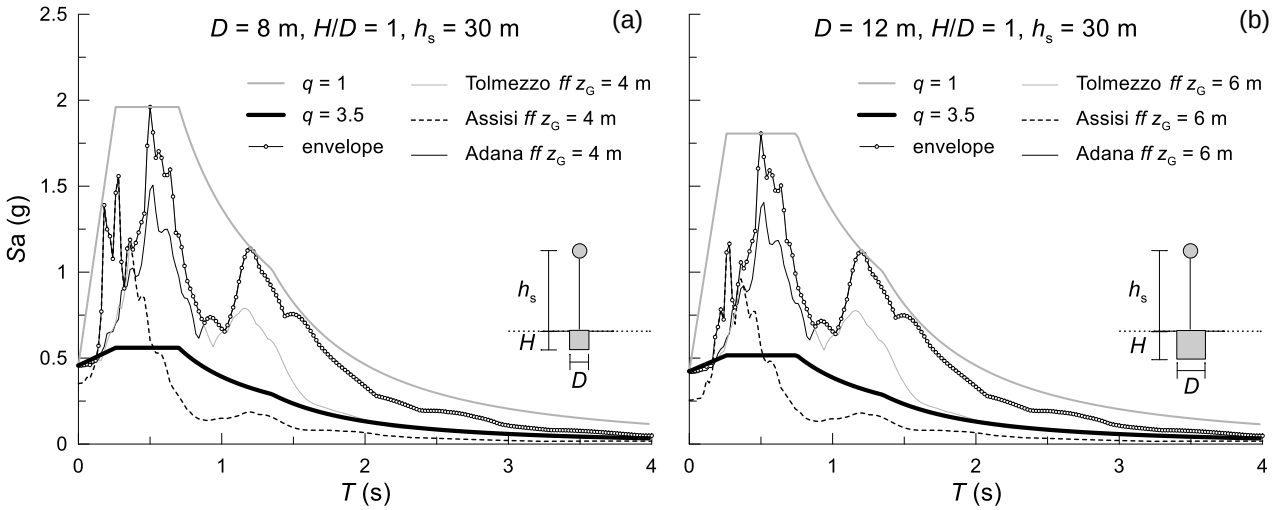

Fig. 14. Elastic acceleration spectra for the piers with h_s = 30 m supported by caissons with slenderness ratio H/D = 1 and (a) D = 8 m; (b) D = 12 m, adopting the first set of input motions.

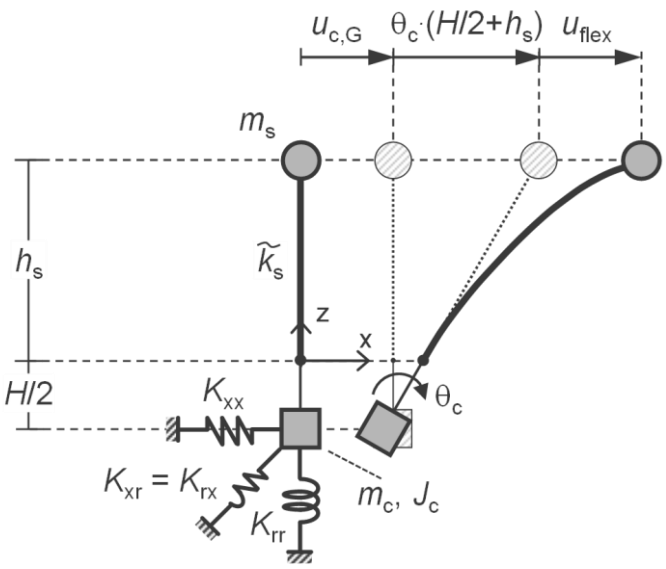

Fig. 15. Kinematics of the 3 degrees of freedom systems modelled in the FE code SAP2000 v.16 [38].